IEEE Access
Multidisciplinary | Rapid Review | Open Access Journal

Received May 29, 2018, accepted June 24, 2018, date of publication July 4, 2018, date of current version July 30, 2018.

Digital Object Identifier 10.1109/ACCESS.2018.2852801

A Study on the Transient of Secondary Arc Current of UHV Transmission Lines

QIUQIN SUN[1], (Member, IEEE), ZHIBIN XIAO[1], HONGSHUN LIU[2], QINGMIN LI[3], (Member, IEEE), AND FENG WANG[1]

[1]College of Electrical and Information Engineering, Hunan University, Changsha 410082, China
[2]School of Electrical Engineering, Shandong University, Jinan 250061, China
[3]School of Electrical and Electronic Engineering, North China Electric Power University, Beijing 102206, China

Corresponding author: Qiuqin Sun (sunqq@hnu.edu.cn)

This work was supported by the National Natural Science Foundation of China under Grant 51507058.

ABSTRACT Secondary arcs are a type of alternating-current electric arc burning in open space, the arcing times of which are closely related to the transient of their currents. To elucidate the formation mechanism of the transient, the secondary current was first decomposed into the natural component and the forced component. Then, the corresponding circuit models were established and the formulas calculating these two components were derived. By means of the electromagnetic transients program simulation, the typical secondary arc current waveform is gotten, and its evolution is divided into three stages based on its characteristics. The influences of key factors (e.g., secondary arc resistance, shunt compensation degree, and neutral reactor) on the transient were investigated, and the most critical factor was obtained. It indicates that the transient of secondary arc current is mainly characterized by its natural component. Furthermore, using the Laplace transform method, and along with the simplification of the system circuit, the characteristic equation for the UHV transmission line was developed, and the damping factors and resonant frequencies of the natural component were solved. Compared with the previous steady-state analysis, the relationship between the decaying and oscillating processes with the system parameters is quantitatively explained. Rather than the line length, the neutral reactor, the decay of secondary arc current is directly proportional to the arc resistance, but inversely proportional to shunt reactor. The proposed methodology can be also applied to recovery voltage study. The results are essential for the transient analysis, the choice of neutral reactor, as well as the implementation of single-phase auto-reclosing strategy.

INDEX TERMS Ultra high voltage, secondary arc current, four-reactor bank scheme, Laplace transform method, natural component, forced component.

I. INTRODUCTION

Single-phase auto-reclosing (SPAR) is widely used in UHV transmission lines to improve the transient stability of power systems [1]. After a grounding fault on a UHV transmission line, the faulted phase should be rapidly cleared; then, a secondary arc occurs due to the capacitive and inductive coupling from the adjacent sound phases. The secondary arc is one of the crucial technical challenges for UHV power transmission due to the extremely high voltage and the long span. If it is not extinguished within the prescribed time, the circuit breakers of the faulted phase would be reclosed on the fault, damaging the associated power equipment and even leading to the out of step of the power system [1]–[3].

The secondary arc is a highly complex phenomenon and the affected by various factors [4]–[6]. Since the1960s, with the development of extra high voltage (EHV) transmission systems, extensive research has been carried out on its physical mechanism, mathematical modelling and extinguishing techniques. Electric utilities of America, Russia, China, Japan and Brazil conducted numerous tests on the secondary arc to investigate the characteristics of its arcing time and thereby to determine the dead time of EHV and UHV transmission lines. The arc was captured, and its voltage and current were recorded and analysed in detail [7]–[12]. Supposing the secondary arc body as a chain, the mechanical forces acting on secondary arc column have been modelled and comprehensively discussed. Both the thermal effect and wind on secondary arc are taken into account [5]. Based on the experimental results, the theory of switching arc is extended to model an unconstrained long fault arc in air, and a number

of black-box models for secondary arc have been proposed and incorporated into the electromagnetic transients program (EMTP) [9], [13]. It should be noted that the arcing time is random and of statistics in practice; the existing models have certain limitations, for instance, most of models are suitable for some given cases and conditions only; the dielectric strength of free air is extremely difficult to determine [13].

Meanwhile, several extinguishing techniques for the secondary arc have been proposed [1], [14], [15]. Knudsen first presented the four-reactor bank scheme, which not only compensate the reactive power but also eliminate the capacitive coupling between phases and thus reduce the secondary arc current significantly. This method has been widely employed in existing EHV and UHV transmission lines. Hasibar introduced the high speed grounding switch, which is currently applied to the short UHV transmission lines of Japan; Shperling proposed a modified selective switched four-reactor scheme, and this technique is especially suitable for untransposed lines where the conventional techniques cannot minimize the secondary arc current effectively.

The secondary arc is an alternating current electric arc in essence, which is generally extinguished when its current crosses zero, and hence its arcing time is closely related to the transient of its current. Most of previous studies are performed from the perspective of steady-state analysis. By means of EMTP simulation, the variations of steady-state current versus the system parameters, like the neutral reactor, line length and arc resistance are obtained [16]. Currently, the choice of neutral reactor value is also based on the steady-state analysis. In order to determine the SPAR strategy, several researchers have investigated the characteristics of the transient [17], [18]. Using the adaptive cumulative sum method, the successive events are identified and the fault types are distinguished; the harmonic content of terminal voltage is employed as a sign to evaluate the stage for fault. However, presently little attention has been paid to the detailed interaction between the line parameters and the transient; the mathematical relationship between these variables are unknown; the formation mechanism of such transient is still not clearly understood so far, and that is the main objective of this work.

II. CALCULATION FOR SECONDARY ARC CURRENT

A. EQUIVALENT CIRCUIT FOR SECONDARY ARC CURRENT

Secondary arc currents are caused by the capacitive and inductive couplings from adjacent sound phases of a transmission line. The inductive coupling, which contributes little to the current [19], is ignored in this work to facilitate the analysis.

The circuit diagram for UHV transmission line is illustrated in Fig. 1. For the purpose of reactive power compensation, shunt reactor banks, as represent by L_P, are normally installed on the ends of the line. A small reactor, as represented by L_N, is often connected to the linking point of the banks to eliminate the capacitive coupling between phases.

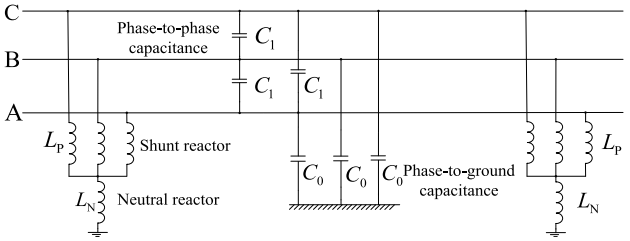

FIGURE 1. Circuit diagram for UHV transmission line.

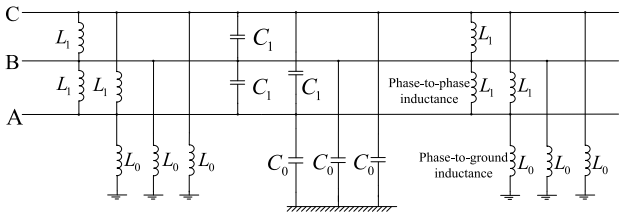

FIGURE 2. Equivalent circuit diagram for UHV transmission line. L_0 is the equivalent phase-to-phase inductance; L_1 is the equivalent phase-to-ground inductance.

The diagram can be easily converted into Fig. 2.The equivalent phase-to-phase L_0 and the phase-to-ground inductance L_1 can be easily derived.

$$\begin{cases} L_0 = L_P + 3L_N \\ L_1 = \dfrac{L_P}{L_N}(L_P + 3L_N) \end{cases} \tag{1}$$

The line susceptance and shunt compensation degree are given in (2).

where B_1 is the positive-sequence susceptance, B_0 is the zero-sequence susceptance, F is the shunt compensation degree; X_r is the equivalent reactance of line shunt reactor.

In order to minimize the capacitive coupling between phases,

$$\begin{cases} B_1 = \omega \dfrac{C_0 C_1}{C_1 + 2C_0} \\ B_0 = \omega \dfrac{C_0 C_1}{C_1 - C_0} \\ F = \dfrac{1}{X_r \cdot B_1} \end{cases} \tag{2}$$

the L_1-C_1 branches shown in Fig.2 must resonate. To achieve this, the neutral reactor should satisfy [19]

$$X_n = \frac{B_1 - B_0}{3F \cdot B_1 \cdot [B_0 - (1 - F) \cdot B_1]} \tag{3}$$

B. COMPOSITION OF SECONDARY ARC CURRENT

Under normal conditions, the voltage and current of each element in a circuit vary periodically. When a single phase-to-ground fault takes place, the faulted phase would be cleared in 2-3 cycles of fundamental frequency and the secondary arc then occurs. According to the superposition theorem [20], the secondary arc generally consists of two parts, i.e., the

natural component and the forced component:

$$i(t) = i_{\mathrm{n}}(t) + i_{\mathrm{f}}(t) \tag{4}$$

where the subscripts n and f denote natural and forced, respectively.

The forced component $i_{\mathrm{f}}(t)$ is a response of the circuit to the power sources. It is a sinusoid and can be expressed as

$$i_{\mathrm{f}}(t) = I_{\mathrm{f}} \sin(\omega_0 t + \varphi_0) \tag{5}$$

where I_{f} is the magnitude, ω_0 is the power angular frequency, φ_0 is the initial phase angle.

The natural component $i_{\mathrm{n}}(t)$ is a response of the circuit to the energy stored in the inductors and capacitors at the moment the circuit breakers of the faulted phase are cleared [18]. It is a sum of several exponentially decaying terms and can be expressed as

$$i_{\mathrm{n}}(t) = \sum_{i=1}^{m} I_{\mathrm{i}} e^{\delta_{\mathrm{i}} t} \cos(\omega_{\mathrm{i}} t + \varphi_{\mathrm{i}}) + I_0 \tag{6}$$

where

m is the order of the natural component;
I_{i} is the magnitude of the i^{th} term;
δ_{i} is the damping factor of the i^{th} term;
ω_{i} is the resonant frequency of the i^{th} term;
φ_{i} is the initial phase angle of the i^{th} term;
I_0 is the DC component.

The variables δ_{i} and ω_{i} are the two critical quantities featuring the natural component. The former indicates the decaying rate whereas the latter indicates the oscillating rate. Due to the presence of the term $e^{\delta_{\mathrm{i}} t}$, the natural component would decay until zero as time goes on.

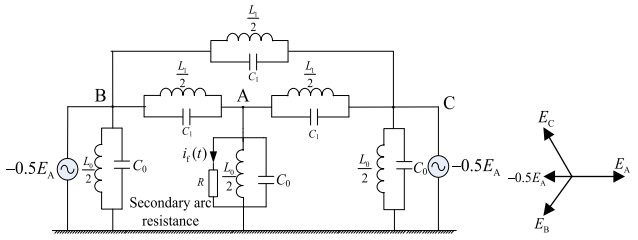

FIGURE 3. Equivalent circuit diagram for forced component.

C. CALCULATION FOR FORCED COMPONENT

Supposing a fault occurs on phase A, the equivalent circuit for the forced component can be reduced to Fig. 3 [1]. Due to symmetry, phase B and C can be folded together and the diagram can be further simplified, as shown in Fig. 4. The impedances Z_0 and Z_1 are equal to

$$\begin{cases} Z_0 = \dfrac{\mathrm{j}\omega L_0}{2 - \omega^2 L_0 C_0} \\ Z_1 = \dfrac{\mathrm{j}\omega L_1}{4 - 2\omega^2 L_1 C_1} \end{cases} \tag{7}$$

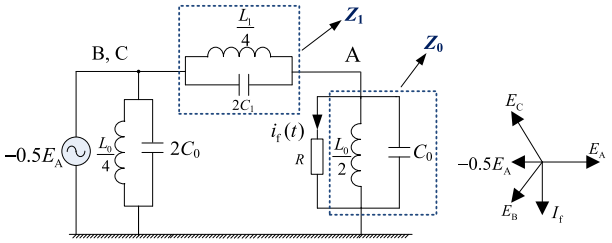

FIGURE 4. Simplified circuit diagram for forced component.

Generally, Z_0 and Z_1 are much greater than the secondary arc resistance R. Thus, the forced component is approximately equal to

$$I_{\mathrm{f}} \approx \frac{-0.5E_{\mathrm{A}}}{Z_1} \tag{8}$$

Since the compensation degree of UHV transmission lines is normally designed in the range from 60% to 90%, Z_1 is capacitive. Hence, the forced component, as shown in the phasor diagram of Fig. 4, always lags E_{A} by 90°.

Clearly, the forced component is heavily dependent on the voltage level of the power sources, the parameters of the shunt reactors and the neutral reactor. The arc resistance, phase-to-ground capacitances, etc., however, have little effect on it.

D. CALCULATION FOR NATURAL COMPONENT

The LTM is a technique for solving linear differential equations with initial conditions. It is able to convert equation in time domain into frequency domain, and commonly used to solve electric circuit and systems problem. The LTM is especially suitable for the calculation of natural component of secondary arc current and determine the quantitative relationship between the transients and the line parameters [20]. Supposing the circuit breakers of the faulted phase are tripped at t_0, the equivalent circuit diagram for the natural component is illustrated in Fig. 5.

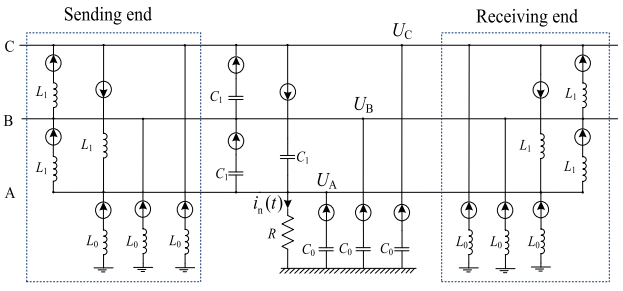

FIGURE 5. Equivalent circuit diagram for natural component. The symbols represent the equivalent voltage sources of the elements.

According to Kirchhoff's voltage law (KVL), the voltage of each node satisfies

$$\begin{bmatrix} Y_{AA} & Y_{AB} & Y_{AC} \\ Y_{BA} & Y_{BB} & Y_{BC} \\ Y_{CA} & Y_{CB} & Y_{CC} \end{bmatrix} \begin{bmatrix} U_A \\ U_B \\ U_C \end{bmatrix} = \begin{bmatrix} I_A \\ I_B \\ I_C \end{bmatrix} \tag{9}$$

The elements of the admittance matrix $\boldsymbol{Y}$ are given in (10).

$$\begin{cases} Y_{AA} = \dfrac{2}{L_0 s} + \dfrac{4}{L_1 s} + 2C_1 s + C_0 s \\ Y_{BB} = \dfrac{2}{L_0 s} + \dfrac{4}{L_1 s} + 2C_1 s + C_0 s \\ Y_{CC} = \dfrac{1}{R} + \dfrac{2}{L_0 s} + \dfrac{4}{L_1 s} + 2C_1 s + C_0 s \\ Y_{AB} = Y_{BA} = -\left(\dfrac{2}{L_1 s} + C_1 s\right) \\ Y_{AC} = Y_{CA} = -\left(\dfrac{2}{L_1 s} + C_1 s\right) \\ Y_{BC} = Y_{CB=} - \left(\dfrac{2}{L_1 s} + C_1 s\right) \end{cases} \tag{10}$$

The elements of the current vector $\boldsymbol{I}$ are given in (11).

$$\begin{cases} I_A = -u_{A-B}(t_0)\, C_1 + u_{C-A}(t_0)\, C_1 + u_A(t_0)\, C_0 \\ \quad + \dfrac{-i_{A-B-S}(t_0) + i_{C-A-S}(t_0) + i_{A-S}(t_0)}{s} \\ \quad + \dfrac{-i_{A-B-R}(t_0) + i_{C-A-R}(t_0) + i_{A-R}(t_0)}{s} \\ I_B = -u_{B-C}(t_0)\, C_1 + u_{A-B}(t_0)\, C_1 + u_B(t_0)\, C_0 \\ \quad + \dfrac{-i_{B-C-S}(t_0) + i_{A-B-S}(t_0) + i_{B-S}(t_0)}{s} \\ \quad + \dfrac{-i_{B-C-R}(t_0) + i_{A-B-R}(t_0) + i_{B-R}(t_0)}{s} \\ I_c = -u_{C-A}(t_0)\, C_1 + u_{B-C}(t_0)\, C_1 + u_C(t_0)\, C_0 \\ \quad + \dfrac{-i_{C-A-S}(t_0) + i_{B-C-S}(t_0) + i_{C-S}(t_0)}{s} \\ \quad + \dfrac{-i_{C-A-R}(t_0) + i_{B-C-R}(t_0) + i_{C-R}(t_0)}{s} \end{cases} \tag{11}$$

where S and R denote sending end and receiving end, repsectively. The current $i_{A-B-S}(t_0)$ represents the instantaneous current of the mutural inductor between phase A and B at t_0; the voltage $u_{A-B}(t_0)$ represents the instantaneous voltage of the mutal capacitor between phase A and B at t_0.

The natural component of secondary arc current is

$$i_{\mathrm{n}}(\mathrm{s}) = \frac{U_{\mathrm{A}}}{R} \tag{12}$$

Through Inverse Laplace Transform, we obtain

$$i_{\mathrm{n}}(\mathrm{t}) = \mathcal{L}^{-1}\left(\frac{U_{\mathrm{A}}}{R}\right) \tag{13}$$

After clearing the faulted phase, the energy stored in the phase-to-phase capacitors, phase-to-ground capacitors, shunt reactors, etc., would be released through the secondary arc path and hence the natural component is generated. Rather than the voltage level of the power sources, the natural component is mainly determined by the initial condition when the circuit breakers are tripped and the configuration of the circuit itself. The secondary arc can damp the natural component and dissipate the energy. As time goes on, the natural component would die out.

III. SIMULATION AND DISCUSSION

In this section, a model for a practical UHV transmission line is established, and the characteristics of secondary arc current are systematically studied.

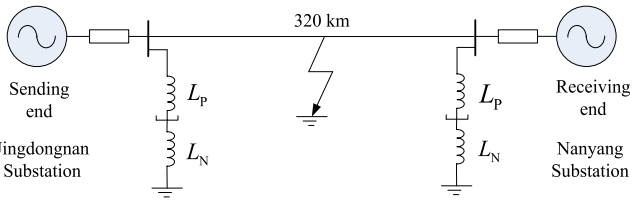

FIGURE 6. Simulation model for UHV transmission line.

A. SIMULATION

In order to analyse the transient of secondary arc current, a practical UHV transmission line of China was selected, i.e. the Jingdongnan-Nanyang line. The simulation model, as illustrated in Fig. 6, was established in the environment of EMTP.

TABLE 1. Parameters of UHV transmission line.

Quantity	Value	Quantity	Value
R_1	0.0081Ω/km	R_0	0.2149Ω/km
L_1	0.8376mH/km	L_0	2.3493mH/km
C_1	0.0138μF/km	C_0	0.0092μF/km

TABLE 2. Equivalent impedances of powersources.

Power source	Quantity	Value
Sending end	Z_1	0.80+j0.879 Ω
	Z_0	0.86+j52.752 Ω
Receiving end	Z_1	3.15+j8.164 Ω
	Z_0	5.69+j14.192 Ω

The UHV transmission line is 320 km in length, fully transposed, and its parameters are listed in Table 1. By means of the short-circuit study, the equivalent impedances of the power sources was obtained, as listed in Table 2. The subscripts 0 and 1 denote zero sequence and positive sequence, respectively. Four-reactor banks are installed on the ends of

the line with total compensation degree of 90%. The neutral reactor is designed as 1390 mH to fully compensate the capacitive coupling between phases.

The secondary arc is a highly complex phenomenon and is affected by various factors, such as the wind, the primary arc and the structure of insulator string [4]–[6]. As a result, its resistance varies in a wide range. Although a number of models have been proposed on its dynamics, its physical mechanism is still not clearly understood. Moreover, due to its extremely random characteristics, it is difficult to reproduce the arc behaviour accurately. In this work, a simplified model is employed to represent the arc and its resistance is set to be a constant of 10 Ω. It should be noted that such a simplification might lead to a slight difference between the simulation results and the experimental results, and the extinguishment and restrike behaviours cannot be simulated. However, the feature of transient can still be demonstrated. In addition, the formulas describing the relationship between the transient and the arc resistance can be obtained, elucidating the formation mechanism of secondary arc current. The influence of the arc resistance is systematically analysed in Sections IV and V.

Assuming that a single phase-to-ground fault occurs on the midpoint of the transmission line at $t = 0.4$ s and the faulted phase is cleared after 60 ms, the results are as follows.

B. RESULTS AND DISCUSSION

A typical secondary arc current is depicted in Fig. 7. Since the simplified linear model is employed to represent the secondary arc resistance, the waveform is slightly different from that measured during field tests.

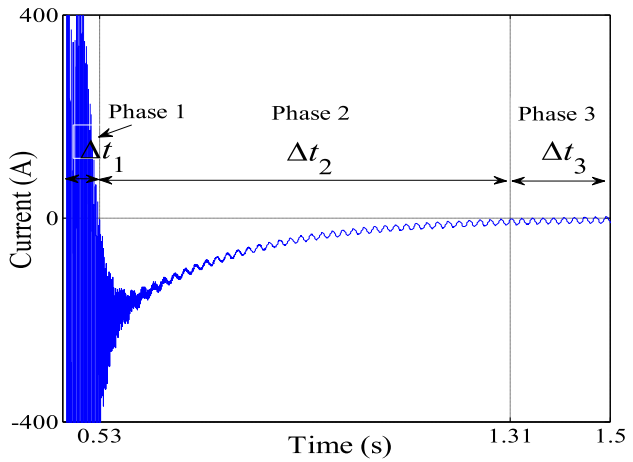

FIGURE 7. Secondary arc current.

It can be seen that the current varies drastically during the early stage with maximum value above 400 A; it decreases towards zero as time goes on. Based on its characteristics, the current can be divided into three phases:

Phase 1: the oscillating phase. It can be easily seen that that the secondary arc current contains a large proportion of high frequency components which oscillates quite rapidly. The duration of phase 1 is 0.07 s, from $t = 0.46$ s, at the moment the current occurs, to $t = 0.53$s, at the moment the current crosses zero for the last time during the early stage.

Phase 2: the decaying phase. As shown in Fig. 7, there is a dc component in the secondary arc current which decays slowly and hence delays the zero-crossing time of the current. The duration of phase 2 is 0.78 s, from 0.53 s when the current crosses zero, to 1.31 s when the dc component has died out and the current crosses zero again.

Phase 3: the steady-state phase. Both the high frequency and dc components have died out, and the secondary arc current is in steady state with effective value about 4 A.

From above results, it can be found that:

- The application of the four-reactor bank can reduce the steady-state value of the secondary arc current significantly.
- The transient of secondary arc current is totally different from its steady state. The transient analysis should be performed to determine the arcing time of the secondary arc, the SPAR strategy as well as the transmission line design.
- The secondary arc is a long alternating-current electric arc in nature, which is generally extinguished when its current crosses zero. As shown in Fig. 7, the duration of phase 2, which is without zero-crossing point, reaches almost 0.8 s. However, to ensure the transient stability of power systems, the dead time of a UHV transmission line is normally within 1 s, including the tripping delay, the interrupting time of circuit breakers, the arcing time of the fault arc, etc [18]. It suggests that the arcing time may even exceeds the dead time of the line, resulting in the failure of SPAR. The presence of the DC content poses a threat to the arc extinction.
- The entire trend of the transient is similar to those of the experimental results presented in [7]–[12]. However, compared with experimental results, the secondary arc current of our case decays rather slowly. Such a difference is explained in the following sections.

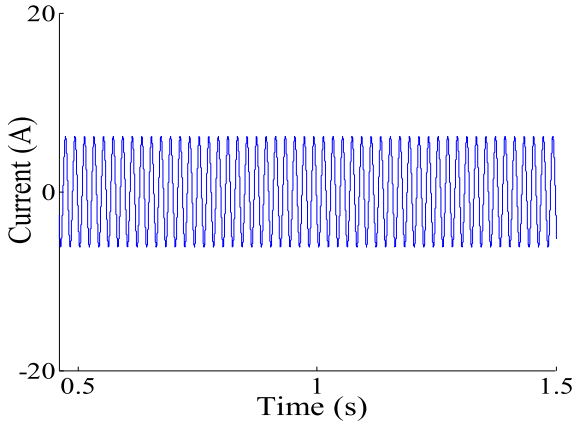

FIGURE 8. Forced component.

The secondary arc current was decomposed, and its two components are depicted in Fig 8 and 9, respectively.

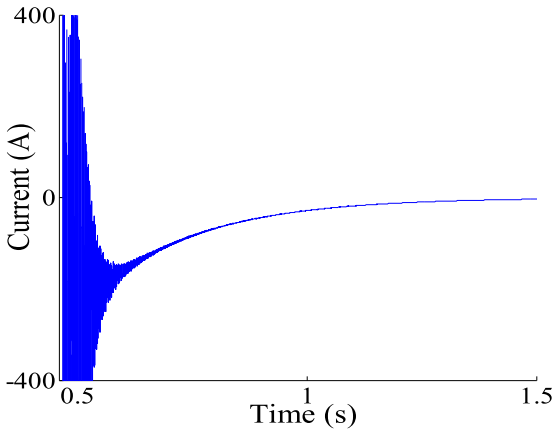

FIGURE 9. Natural component.

The forced component is a sinusoid with effective value of 4.3 A whereas the natural component is similar to the total current. Apparently, the natural component is considerably higher than the forced component. It consists of a variety of harmonics, including high frequency harmonics, low frequency harmonics and a DC content. They decay towards zero as time goes on. It can be also found that the transient of secondary arc current is mainly featured by its natural component rather than the forced component.

IV. INFLUENCES OF KEY FACTORS ONTHE TRANSIENTST OF SECONDARY ARC CURRENT

To determine the effects of key factors on the transient of secondary arc current, a series of simulations have been performed in this section.

A. INFLUENCE OF SECONDARY ARC RESISTANCE

The variations of forced component and natural component with the secondary arc resistance are shown in Fig. 10 and 11, respectively.

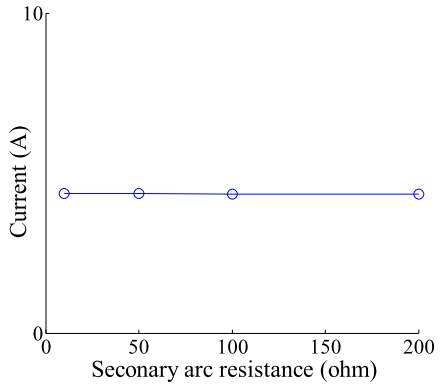

FIGURE 10. Forced component versus secondary arc resistance.

Since the forced component is a sinusoid, which is mainly characterized by its effective value, instead of the whole waveform, only the effective value is presented here for the analysis. The forced component is 4.3 A when the resistance

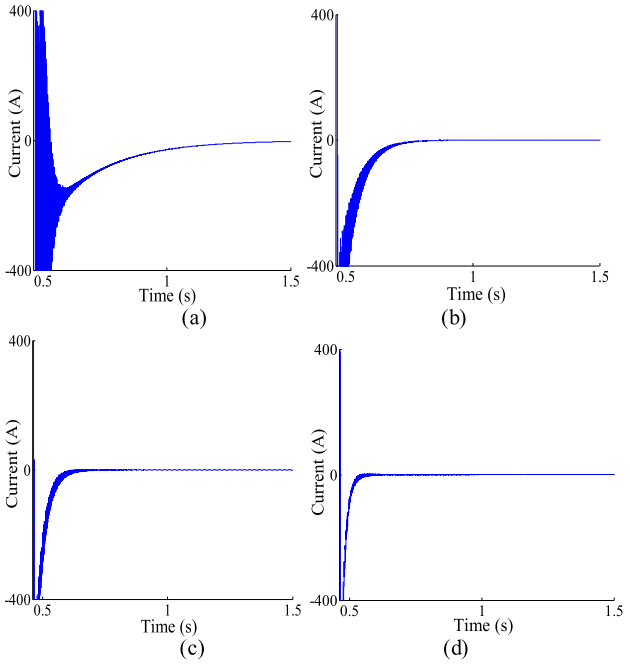

FIGURE 11. Natural component versus secondary arc resistance (a) R=10 Ω. (b) R=50 Ω. (c) R=100 Ω. (d)R=200 Ω.

is 200 Ω, and it almost keep constant with the increase of the resistance. Since the arc resistance is much smaller than the equivalent impedance between the healthy phase and the fault point, from Fig. 10, it can be seen that the resistance has little effect on the forced component. This result is consistent with the theoretical analysis presented in Section II and the results presented in [21].

However, the natural component, as shown in Fig. 11, is significantly influenced by the secondary arc resistance. The greater the resistance is, the faster the decay will be. When the resistance is 10 Ω, the natural component dies out up to 0.8 s but within 0.2 s when it is 200 Ω. In practice, the voltage on the faulted phase of a transmission line are usually measured and analysed to identify whether the fault is transient or permanent, and thus to determine the SPAR strategy. The information of the transient is meaningful and of great significance. The simulation results indicate that the modelling of the secondary arc resistance is essential to SPAR strategy, and our analysis are more comprehensive than previous study.

B. INFLUENCE OF COMPENSATION DEGREE

The variations of forced component and natural component with the degree of shunt compensation are plotted in Fig. 12 and 13, respectively.

From Fig. 12, it can be seen that the effective value of the forced component is 12.2 A when the compensation degree is 60%, but 4.3 A when it is 90%. Clearly, the compensation degree has small effect on the forced component when it is less than 80%. When the degree exceeds 80%, the forced component goes down rapidly with the increase of the shunt compensation degree.

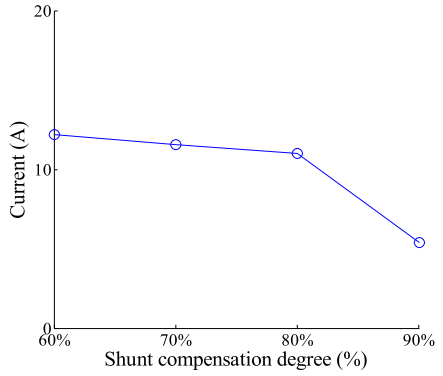

FIGURE 12. Forced component versus shunt compensation degree.

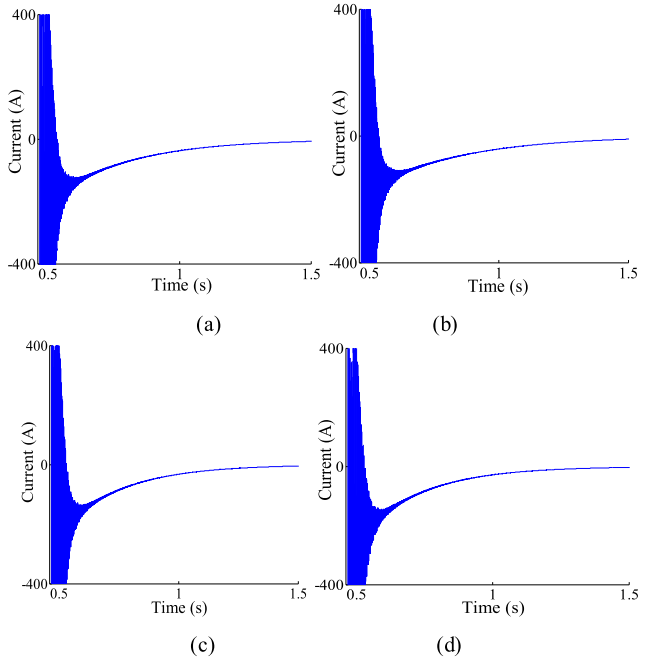

FIGURE 13. Natural component versus compensation degree (a) T=60%. (b) T=70%. (c) T=80%. (d) T=90%.

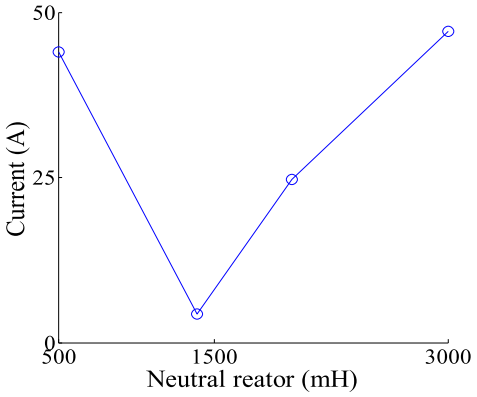

FIGURE 14. Forced component versus neutral reactor.

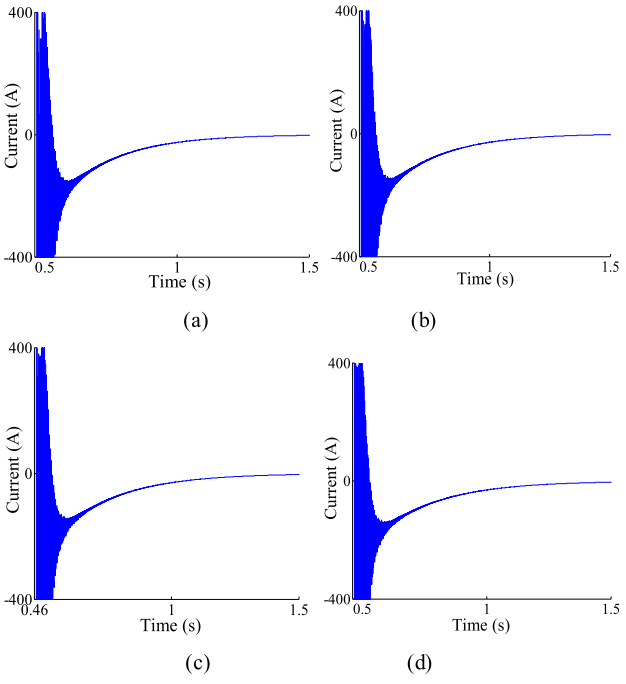

FIGURE 15. Natural component versus neutral reactor (a) Ln=500 mH. (b) Ln=1390 mH. (c) Ln=2000 mH. (d) Ln=3000 mH.

Similarly, the compensation degree, as shown in Fig. 13, has little influence on the natural component, and it decays relatively faster when the shunt compensation degree is high. In the case that one of the shunt reactor banks is out of service, the natural component would not be significantly affected.

C. INFLUENCE OF NEUTRAL REACTOR

The effects of neutral reactor on the forced component and natural component are shown in Fig. 14 and 15, respectively.

Regarding the forced component, its value is determined by the ratio of the secondary arc resistance to the equivalent impedance between the healthy phase of circuit and the fault. The use of neutral reactor can compensate the capacitive coupling between phases, and once the phase-to-phase inductance and the phase-to-phase capacitance reach the resonant condition, the impedance has the maximum and the forced component would have its minimum. The neutral rector has a great impact on the impedance and thus the forced component. Form Fig. 14, it can be seen that the minimum value of forced component is 4.3 A when the neutral reactor is 1390 mH. When the reactor is smaller than 1390 mH, the forced component decreases rapidly with the increase of the reactor, and vice versa. Thus, the selection of an appropriate neutral reactor is crucial to ensure that the secondary arc current is deeply suppressed below an acceptable level.

The natural component, however, is mainly characterized by the decay and oscillating features. The damping factor, which is determined by the time constant of the circuit, is primarily related to the secondary arc resistance; the variation of neutral reactor would not change the order of the circuit. As shown in Fig. 15, the influence of neutral reactor on the natural component is quite small, and the waveform nearly keeps the same with the increase of the reactor.

D. INFLUENCE OF FAULT LOCATION

The variations of forced component and natural component with fault location are shown in Fig. 16 and 17, respectively.

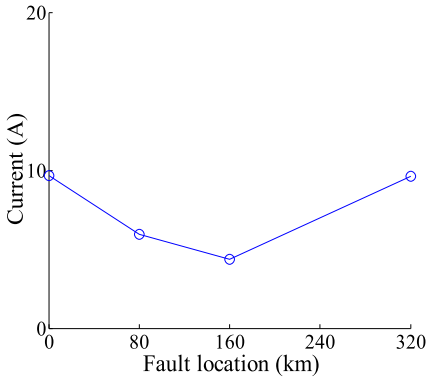

FIGURE 16. Forced component versus fault location.

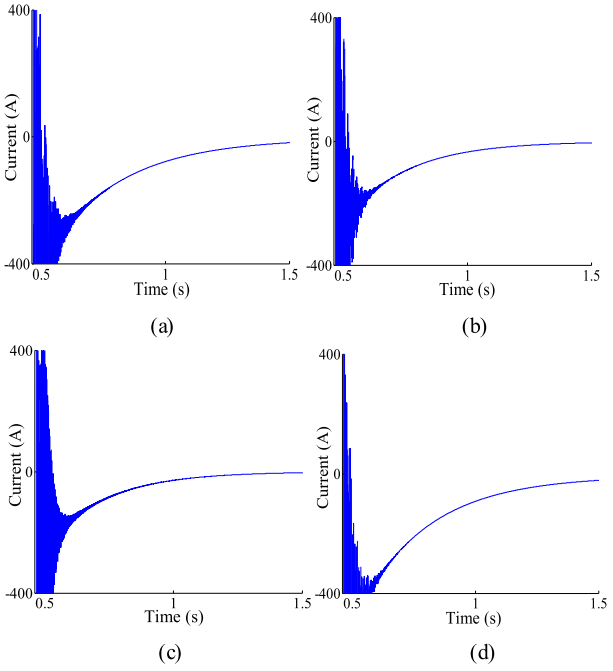

FIGURE 17. Natural component versus fault location (a) L=0 km. (b) L=80 km. (c) L=160 km. (d) L=320 km.

Clearly, the fault location has little effect on the forced component. When the fault is located at 160 km, the forced component is 4.8 A but 10.2 A at the receiving end. The influence of fault location on the natural component is also fairly small. Generally, the component decays faster when the fault location approaches the midpoint of the line.

From above results, it can be concluded:

- The forced component is mainly determined by the neutral reactor. In order to minimize the steady-state value of secondary arc, the selection of the neutral reactor is crucial.
- The natural component is heavily dependent on the secondary arc resistance. Since the voltage of a faulted phase is often used as an input signal for a SPAR scheme, it is necessary to simulate the secondary arc resistance to obtain the accurate waveform of the voltage.

V. DECAYING AND OSCILLATING CHARACTERISTICS OF NATURAL COMPONENT

The aforementioned analysis indicates that the transient of secondary arc current is mainly characterized by its natural component, and this component is decided by the secondary arc resistance. In this section, the formation mechanism of the natural component is further elucidated.

A. CHARACTER IS TIC EQUATION OF CIRCUIT

The decay and oscillation are two crucial attributes properties describing the natural component. The characteristic equation is an effective method to calculate the damping factors and resonant frequencies of a circuit. Taken the source impedances into account, the equivalent circuit model for the natural component is illustrated in Fig. 18. This model can be further reduced into Fig. 19 [21].

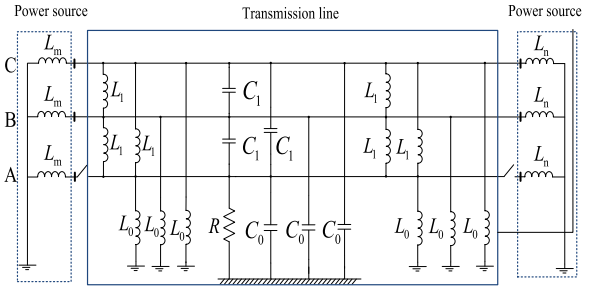

FIGURE 18. Circuit diagram for the characteristic equation.

Using LTM, Z_1, Z_2 and Z_3 are converted into the frequency domain, as given in (14)

$$\begin{cases} Z_1 = \dfrac{sL_1}{4 + 2s^2 L_1 C_1} \\ Z_2 = \dfrac{s\,(2L_m + 2L_n + L_0)}{4 + 2s^2\,(2L_m + 2L_n + L_0)\,C_0} \\ Z_3 = \dfrac{sL_0}{2 + s^2 L_0 C_0} \end{cases} \tag{14}$$

And,

$$Z_{eq} = \frac{(Z_1 + Z_2) \times Z_3}{Z_1 + Z_2 + Z_3} \tag{15}$$

The characteristic equation of the circuit is

$$R + Z_{eq} = 0 \tag{16}$$

Equation (13) can be written in the form

$$a_4 s^4 + a_3 s^3 + a_2 s^2 + a_1 s + a_0 = 0 \tag{17}$$

where a_0, a_1, a_2, a_3 and a_4 are constants determined by the parameters of the elements in the circuit.

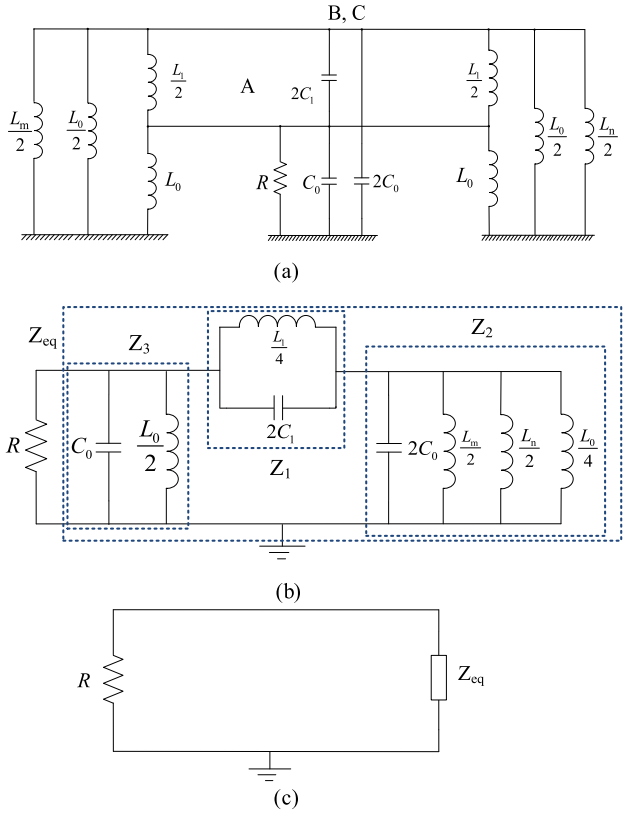

FIGURE 19. Simplification of circuit (a) Original circuit (b) Preliminary reduced circuit (c) Further reduced circuit.

B. DAMPING FACTOR AND RESONANT FREQUENCY OF NATURAL COMPONENT

Substituting the parameters of the transmission line into (14), the normalized coefficients of the equation are obtained, as listed in Table 3. It can be seen that the characteristic equation is a fourth-order polynomial equation, and it contains fours roots, as listed in Table 4.

TABLE 3. Coefficients of characteristic equation.

Coefficient	Value
a_0	1
a_1	133
a_2	135
a_3	110
a_4	123

The natural component can be expressed as

$$i_n(t) = b_1 e^{s_1 t} + b_2 e^{s_2 t} + + b_3 e^{s_3 t} + + b_4 e^{s_4 t} \quad (18)$$

TABLE 4. Roots of characteristic equation.

Root	Value
s_1	-50.18+j5299.48
s_2	-50.18-j5299.48
s_3	-38669.28
s_4	-3.08

where b_1, b_2, b_3 and b_4 are constants determined by the initial condition when the faulted phase is cleared.

The roots suggests that the natural component can be divided into three parts: (i) the slowly decaying but rapidly oscillating part, as indicated by the roots s_1 and s_2 whose damping factors are fairly small but resonant frequencies are very large; (ii) the rapidly decaying part, as indicated by the root s_3 whose damping factor are much greater than those of others; (iii) the slowly decaying part, as indicated by the root s_4 whose damping factor is extremely small. It can be observed that the damping factor of s_4 is far smaller than those of others; hence, it would play a decisive role in the decay of the total natural component.

Comparing the roots with the waveform depicted in Fig. 7, it can be inferred that the roots s_1, s_2 and s_3 as well as their term presented in (15) correspond to Phase 1, and the root s_4 as well as its term $b_4 e^{s t}_4$ corresponds to Phase 2.

TABLE 5. Roots of the characteristic equation.

Root	Value
s_1	-115.29+j5627.06
s_2	-115.29+j5627.06
s_3	-1694.04
s_4	-64.01

C. INFLUENCES OF KEY FACTORS ON THE ROOTS

Table 5 lists the roots of the characteristic equation with secondary arc resistance of 200 Ω. Compared with Table 4, it is clearly that the damping factors of s_1, s_2 and s_4 increase simultaneously with the increase of the secondary arc resistance. It means that a greater arc resistance would lead to a faster attenuation of the natural component. It is worth noting

that that the damping factor of s_4 increases almost linearly with the increase of the secondary arc resistance, and the ratio of these two resistances (200Ω/10Ω) is approximately equal to the ratio of the two damping factors (−64.01/−3.08). It means that the natural component is highly dependent on the secondary arc resistance and this analytical result is consistent with the simulation results.

Generally, the power source impedances L_m and L_n are much smaller than L_0. Neglecting these two impedances, Eq. (15) would be transformed into a quadratic equation and the damping factor of s_4, represented by δ_4, is solved as

$$\delta_4\,(t) \approx -\frac{R\left(2L_p + 4L_n\right)}{L_p\left(L_p + 3L_n\right)} \tag{19}$$

Since L_p is much greater than L_n, we obtain

$$\delta_4\,(t) \approx -\frac{2R}{L_p} \tag{20}$$

It can be found that δ_4 is directly proportional to the secondary arc resistance R but inversely proportional to the shunt reactor L_p. In practice, the compensation degree is normally designed in the range from 60% to 90%. As a consequence, L_p is often limited in a small range. The arc resistance, however, varies drastically, normally ranging from several ohms to thousands ohms. Thus, it would play a decisive role in the damping factor.

TABLE 6. Roots of the characteristic equation.

Root	Value
s_1	-50.13+j5294.99
s_2	-50.13−j5294.99
s_3	-39670.51
s_4	-1.95

Table 6 and 7 lists the roots of the characteristic equation when the compensation degree is 60% and the neutral reactor is 3000 mH, respectively. Compared with Table 4, it can be seen that the roots s_1, s_2 and s_3 almost keep unchanged with the variations of compensation degree and the neutral reactor. There is only a small reduce of s_4 when the compensation degree decreases from 90% to 60%. It indicates these two factors have small effects on the decaying and oscillating characteristics of the natural component. The analytical result also agrees well with the simulation results. This is attributed to the fact that the damping factor is closely related to the time constant of the circuit; the smaller the time constant, the more rapidly the current decreases, that is the faster the response. The variation of neutral reactor cannot change the order of the characteristic equation. Further, as it is smaller than the shunt reactor, its effect is very weak.

TABLE 7. Roots of the characteristic equation.

Root	Value
s_1	s_1=-50.02+j5297.55
s_2	s_2=-50.18−j5297.55
s_3	s_3=-39669.84
s_4	s_4=-2.85

In addition to the current, the transient of recovery voltage can be also obtained by applying the LTM to the circuit similarly. The only difference is that the arc is extinguished and R (see Fig. 18) is approaching infinite, in other words without R. The order of the characteristic equation is 3 (see Eq. 16), which is smaller than that of the secondary arc current. Compared with the current, the results suggest that the recovery voltage is mainly impacted by the four-legged shunt reactor parameters instead of the secondary arc resistance itself.

VI. CONCLUSION

In this work, the transient of secondary arc current has been systematically studied. To elucidate the mechanism of the transient, the secondary arc current has been decomposed into the natural component and the forced component; the corresponding circuits have been established; the formulas for these two components have been derived. Then, a series of simulations on secondary arc current of a practical UHV transmission line have been performed and the influences of key factors have been investigated. Furthermore, using LTM, the characteristic equation of the UHV transmission line is formulated; the damping factors and the resonant frequencies describing the natural component are obtained and their characteristics are researched.

The characteristics of the transient of secondary arc current are completely different from that of its steady state. Compared with previous analysis, the relationship between the decaying and oscillating processes with the system parameters is quantitatively explained. Both the simulations and the theoretical analysis indicate that the transient is characterized by its natural component, which is mainly decided by the factor of secondary arc resistance instead of the line length, the fault location, etc. The decay of secondary arc current is directly proportional to arc resistance, but inversely proportional to shunt reactor. Also, the proposed methodology can be extended to recovery voltage study. The analytical results are consistent with the experiments and provide useful references for the implementation of SPAR strategy and the line design.

REFERENCES

[1] IEEE Power System Relaying Committee Working Group, "Protective relaying performance reporting," *IEEE Trans. Power Del.*, vol. 7, no. 4, pp. 1892–1899, Oct. 1992.
[2] Q. Ma, B. Zheng, L. Ban, and Z. Xiang, "Secondary arc current analysis of an untransposed EHV/UHV transmission line with controllable unbalanced shunt reactor," *IEEE Trans. Power Del.*, vol. 30, no. 3, pp. 1458–1466, Jun. 2015.
[3] J. Schindler, C. Romeis, and J. Jaeger, "Secondary arc current during DC auto reclosing in multisectional AC/DC hybrid lines," *IEEE Trans. Power Del.*, vol. 33, no. 1, pp. 489–496, Feb. 2018.
[4] Y. Goda, S. Matsuda, T. Inaba, and Y. Ozaki, "Forced extinction characteristics of secondary arc on UHV (1000 kV class) transmission lines," *IEEE Trans. Power Del.*, vol. 8, no. 3, pp. 1322–1330, Jul. 2005.
[5] Q. Li, H. Cong, Q. Sun, J. Xing, and Q. Chen, "Characteristics of secondary ac arc column motion near power transmission-line insulator string," *IEEE Trans. Power Del.*, vol. 29, no. 5, pp. 2324–2331, Oct. 2014.
[6] G. Bán, L. Prikler, and G. Bánfai, "Testing EHV secondary arcs," in *Proc. IEEE Porto Power Tech. Conf.*, Porto, Portugal, Sep. 2001, p. 6.
[7] T. Tsuboi, J. Takami, S. Okabe, K. Aoki, and Y. Yamagata, "Study on a field data of secondary arc extinction time for large-sized transmission lines," *IEEE Trans. Dielectr. Electr. Insul.*, vol. 20, no. 6, pp. 2277–2286, Dec. 2013.
[8] A. J. Fakheri, T. C. Shuter, J. M. Schneider, and C. H. Shih, "Single phase switching tests on the AEP 765 KV system-extinction time for large secondary arc currents," *IEEE Trans. Power App. Syst.*, vol. PAS-102, no. 8, pp. 2775–2783, Aug. 1983.
[9] I. M. Dudurych, T. J. Gallagher, and E. Rosolowski, "Arc effect on single-phase reclosing time of a UHV power transmission line," *IEEE Trans. Power Del.*, vol. 19, no. 2, pp. 854–860, Apr. 2004.
[10] Y. He, G. Song, and R. J. Cao, "Test research of secondary arc in 1000 kV UHV double-circuit transmission lines," *Proc. CSEE*, vol. 31, no. 16, pp. 138–143, Jun. 2011.
[11] O. Dias, F. Magrin, and M. C. Tavares, "Comparison of secondary arcs for reclosing applications," *IEEE Trans. Dielectr. Electr. Insul.*, vol. 24, no. 3, pp. 1592–1599, Jun. 2017.
[12] M. C. Tavares, J. Talaisys, and A. Camara, "Voltage harmonic content of long artificially generated electrical arc in out-door experiment at 500 kV towers," *IEEE Trans. Dielectr. Electr. Insul.*, vol. 21, no. 3, pp. 1005–1014, Jun. 2014.
[13] A. T. John, R. K. Aggarwal, and Y. H. Song, "Improved techniques for modelling fault arcs an faulted EHV transmission systems," *IEE Proc.-Gener., Transmiss. Distrib.*, vol. 141, no. 2, pp. 148–154, Mar. 1994.
[14] Z. Xu, X. Yan, X. Zhang, and A. Wen, "Compensating scheme for limiting secondary arc current of 1000 kV ultra-high voltage long parallel lines," *IET Gener., Transmiss. Distrib.*, vol. 7, no. 1, pp. 1–8, Jan. 2013.
[15] Q. Sun, J. Yin, F. Wang, J. Yan, Q. Li, and S. Chen, "Influence of grading capacitor of multiple-break circuit breaker on the extinction of secondary arc—A new method for reducing dead time," *IET Gener., Transmiss. Distrib.*, vol. 11, no. 8, pp. 1954–1965, Jun. 2017.
[16] M. C. Tavares and C. M. Portela, "Transmission system parameters optimization-sensitivity analysis of secondary arc current and recovery voltage," *IEEE Trans. Power Del.*, vol. 19, no. 3, pp. 1464–1471, Jul. 2014.
[17] M. Khodadadi, M. R. Noori, and S. M. Shahrtash, "A noncommunication adaptive single-pole autoreclosure scheme based on the ACUSUM algorithm," *IEEE Trans. Power Del.*, vol. 28, no. 4, pp. 2526–2533, Oct. 2013.
[18] S.-P. Ahn, C.-H. Kim, R. K. Aggarwal, and A. T. Johns, "An alternative approach to adaptive single pole auto-reclosing in high voltage transmission systems based on variable dead time control," *IEEE Trans. Power Del.*, vol. 16, no. 4, pp. 676–686, Oct. 2001.
[19] M. R. D. Zadeh, M. Sanaye-Pasand, and A. Kadivar, "Investigation of neutral reactor performance in reducing secondary arc current," *IEEE Trans. Power Del.*, vol. 23, no. 4, pp. 2472–2479, Oct. 2008.
[20] C. K. Alexander and M. N. O. Sadiku, *Fundamentals of Electric Circuits*. New York, NY, USA: McGraw-Hill, 2004.
[21] W. Shi, F. Li, Y. Han, and Y. Li, "The effect of ground resistance on secondary arc current on an EHV transmission line," *IEEE Trans. Power Del.*, vol. 20, no. 2, pp. 1502–1506, Apr. 2005.

QIUQIN SUN (M'14) received the B.Sc. degree in electrical engineering from Chongqing University, Chongqing, in 2006, and the Ph.D. degree in electrical engineering from Shandong University, Jinan, China, in 2012. He joined the Jiangsu Electrical Power Company Research Institute as a Senior Electrical Engineer in 2012. He joined Hunan University, Changsha, China, in 2014, where he is currently an Associate Professor with the College of Electrical and Information Engineering. From 2014 to 2015, he was an Honorary Research Fellow with the University of Liverpool. His research interests include electromagnetic transients of power systems, electric arcs, and intelligent monitoring and diagnostics systems.

ZHIBIN XIAO was born in Changsha, Hunan, China, in 1993. He received the B.Sc. degree in electrical engineering from the Changsha University of Science and Technology, Changsha, China, in 2016.

He is currently pursuing the Ph.D. degree with the College of Electrical and Information Engineering, Hunan University. His research interests include electromagnetic transients of power systems and electric arc.

HONGSHUN LIU received the B.Sc. and Ph.D. degrees from Shandong University, Jinan, China, in 2004 and 2010, respectively. He is currently a Lecturer with the School of Electrical Engineering, Shandong University. His research interests include electromagnetic transients of power systems, electric arcs, and fault current limiters.

QINGMIN LI (M'07) received the B.Sc., M.Sc., and Ph.D. degrees from Tsinghua University, Beijing, China, in 1991, 1994, and 1999, respectively. He is currently a Professor with North China Electric Power University, Beijing, China. His research interests include high-voltage engineering, applied electromagnetics, condition monitoring, and fault diagnostics.

FENG WANG received the B.Sc. degree from Xi'an Jiaotong University, Xi'an, China, in 1994, the M.Sc. degree from Shenyang Polytechnic University, Shenyang, China, in 1999, and the Ph.D. degree from Xi'an Jiaotong University in 2002. He was with Shenyang Transformer, Co., Ltd., as an Electrical Engineer from 1994 to 1996. In 2003, he joined the Darmstadt University of Technology, Germany, as a Post-Doctoral Research Fellow. He joined Hunan University, Changsha, China, in 2004, where he is currently a Professor with the College of Electrical and Information Engineering. His research interests include high-voltage engineering, electric insulation technology, and gaseous dielectrics.